Quasi-Periodicity and Chaos in a Differentially Heated Cavity*

Isabel Mercader

Dep. Física Aplicada. Universitat Politècnica de Catalunya.

Mòdul B4, Campus Nord, 08034 Barcelona, Spain.

Oriol Batiste

Dep. Física Aplicada. Universitat Politècnica de Catalunya.

Mòdul B4, Campus Nord, 08034 Barcelona, Spain.

Xavier Ruiz

Lab. Física Aplicada. Facultat de Ciències Químiques

Univesitat Rovira i Virgili. 43005 Tarragona, Spain

Communicated by

Received date and accepted date

Abstract. Convective flows of a small Prandtl number fluid contained in a two-dimensional vertical cavity subject to a lateral thermal gradient are studied numerically. The chosen geometry and the values of the material parameters are relevant to semiconductor crystal growth experiments in the horizontal configuration of the Bridgman method. For increasing Rayleigh numbers we find a transition from a steady flow to periodic solutions through a supercritical Hopf bifurcation that maintains the centro-symmetry of the basic circulation. For a Rayleigh number of about ten times that of the Hopf Bifurcation, the periodic solution loses stability in a subcritical Neimark-Sacker bifurcation, which gives rise to a branch of quasiperiodic states. In this branch, several intervals of frequency locking have been identified. Inside the resonance horns the stable limit cycles lose and gain stability via some typical scenarios in the bifurcation of periodic

solutions. After a complicated bifurcation diagram of the stable limit cycle of the 1:10 resonance horn, a soft transition to chaos is obtained.

1. Introduction

This work deals with the numerical study of the fluid flows that arise in a two-dimensional cavity, under geometrical conditions and material parameters which are relevant to semiconductor crystal growth according to Bridgman-like techniques. In particular, we consider a laterally heated rectangular cavity under the influence of a vertical gravity field, and we focus on the transitions to time-dependent flows, from periodic oscillations to aperiodic or chaotic motions. The characterization of the different thresholds as well as the different flow regimes become important because of the link between thermal oscillations and solid phase striations, which could damage the crystal quality in a growth process. In the case of a laterally heated cavity, the convective response does not have to overcome a finite threshold, since it occurs for an arbitrarily small Rayleigh number. The successive transitions from the primary convective steady state to the oscillatory and chaotic motions have been the subject of several recent works (Pulicani *et al*., 1990; Le Quéré and Behnia, 1998; Gelfgat *et al*., 1999; Xin and Le Quéré, 2001, among others). These studies have shown a strong dependence on geometrical conditions, on boundary conditions and on material parameters.

One of the dimensionless parameters which affects rather drastically the dynamical behavior of the system, particularly where transition mechanisms to chaos is concerned, is the Prandtl number. Our study will focus on small Prandtl numbers, a parameter region which has not been explored as systematically as others, and which is directly relevant to semiconductor materials. In our simulations we have used the Prandtl number corresponding to molten germanium, $\sigma = 0.00715$. Other works (Braunsfurth *et al*., 1997; Juel *et al*., 2001) have been devoted to studying this problem in three dimensional geometry, but they have been restricted to low values of the Rayleigh number. We have considered horizontal rectangular cavities

⋆ We are particularly grateful to F. Marqués and J. Lopez for their helpful discussions about the work presented here. We would also like to thank L. Ramírez de la Piscina and J. Casademunt. This research has been funded by DGICYT grants BFM2003-00657 and BQU2003-05042-C02-02 . Part of the numerical results were obtained by using the CESCA and CEPBA infrastructure coordinated by C^4.

with aspect ratio 2 (length twice height), with a basic stationary state formed by a single roll. More elongated cells will typically introduce new instabilities which would break the basic roll into more than one (Pulicani *et al.*, 1990). On the other hand, smaller aspect ratios require higher levels of buoyancy for the basic flow to become unstable (Yahata, 1999). Finally, we complete the definition of our physical setup by specifying the boundary conditions. Two fixed temperatures are imposed on the vertical walls, while "perfectly conducting boundaries" are assumed in the horizontal walls. In practice this means that a linear temperature profile is imposed on them. The boundary conditions for the velocity field are no-slip.

In this physical setting, we analyze the nonlinear dynamics when the Rayleigh number varies. After a sequence of bifurcations we obtain a branch of quasiperiodic solutions. Here, we focus on the detailed description of a route to chaos via frequency locking and torus break-down, obtained by increasing the Rayleigh number along this branch. Since the system is invariant under a rotation by π about the center of the cavity, the corresponding symmetry group is $\mathbf{Z}_2$. This group will play an important role in the bifurcation analysis presented below.

The paper is organized as follows. In Sec. 2 we summarize the equations and boundary conditions employed, the symmetries of the problem and their implications, and we discuss the numerical method used. The results obtained by numerical integration of the equations when the Rayleigh number varies are presented in Sec. 3. The paper concludes with a discussion in Sec. 4

2. Mathematical model

We have considered an incompressible fluid in a two-dimensional rectangular cavity of aspect ratio $\Gamma = 2$, where Γ is the ratio between the length d and the height h of the cavity. In the presence of a vertical constant gravity, a temperature difference ΔT is maintained horizontally over the length of the cell, the temperature at the right wall being higher than at the left one. If we nondimensionalize the equations using the height h of the cavity as the unit of length, the imposed lateral temperature difference ΔT as the unit of temperature and the vertical thermal diffusion time $t_T = h^2/\kappa$ (κ is the thermal diffusivity) as the unit

of time, the dimensionless equations in Boussinesq approximation read as follows:

$$\nabla \cdot \mathbf{u} = 0, \tag{1}$$

$$\partial_t \mathbf{u} + (\mathbf{u} \cdot \nabla)\mathbf{u} = -\nabla P + \sigma \nabla^2 \mathbf{u} + \sigma Ra[-0.5 + x/\Gamma + \theta]\hat{\mathbf{z}}, \tag{2}$$

$$\partial_t \theta + (\mathbf{u} \cdot \nabla)\theta = -u/\Gamma + \nabla^2 \theta, \tag{3}$$

here $\mathbf{u} \equiv (u, w)$ is the dimensionless velocity field in (x, z) coordinates, P is the pressure over the density and θ denotes the departure of the temperature from a linear horizontal profile in units of the imposed temperature difference ΔT. The dimensionless parameters are the Prandtl number σ, and the Rayleigh number Ra:

$$\sigma = \frac{\nu}{\kappa}, \quad Ra = \frac{\alpha g h^3}{\nu \kappa} \Delta T,$$

ν denotes the kinematic viscosity, g the gravity acceleration, and α the thermal expansion coefficient.

No-slip boundary conditions have been used on all sides of the cavity, right and left hand sides are maintained at constant temperatures and the horizontal lids are assumed to be perfectly conducting, thus

$$\mathbf{u} = \theta = 0, \qquad \text{at } \partial\Omega. \tag{4}$$

As a measure of the strength of convection, we have used a global variable: the dimensionless quantity

$$E_k = \frac{1}{\Gamma} \int_{x=0}^{x=\Gamma} \int_{z=0}^{z=1} \mathbf{v} \cdot \mathbf{v} \, dx dz,$$

related with the kinetic energy.

Equations together with boundary conditions are invariant under rotations by π about the point $(\Gamma/2, 1/2)$. This rotation can be described by the action of the transformation R defined by

$$R : (x, z) \to (\Gamma - x, 1 - z), \qquad (u, w, \theta) \to (-u, -w, -\theta).$$

Since $R^2 = I$, the R transformation is a generalized reflection, and the resulting symmetry group is $\mathbf{Z}_2 = \{I, R\}$. Two solutions related by transformation R are called R-conjugated. As an indication of the symmetric properties of the solution, we use the value of the local quantity sym defined as the sum of the vertical velocity w in $P_1 = (3\Gamma/4, 3/4)$ and in its centro-symmetric point $P_2 = (\Gamma/4, 1/4)$, i.e., $\mathrm{sym} = w(P_1) + w(P_2)$. If a solution is R-equivariant, $\mathrm{sym} = 0$. The values of sym and E_k for two R-conjugated solutions are opposite and equal, respectively. If $\Psi(t)$ is a periodic solution invariant under R,

the associated periodic orbit is called an *F-cycle*. Periodic solutions, with period T that verify the spacio-temporal symmetry $R\Psi(t) = \Psi(t + T/2)$, are called *symmetric* and the associated periodic orbit is called an *S-cycle*. The cycles corresponding to these solutions are also invariant under R. Since for a *symmetric* solution, $\mathrm{sym}(t) = -\mathrm{sym}(t + T/2)$ and $E_k(t) = E_k(t + T/2)$, we have used the phase diagrams (sym, E_k) to identify these types of cycles; a *symmetric* periodic solution has a phase diagram symmetric with respect to the line $\mathrm{sym} = 0$. A detailed discussion of the codimension 1 bifurcations of equilibria and cycles in $\mathbf{Z}_2$ equivariant systems can be found in Kuznetsov (1985).

We solve equations and boundary conditions using the second order time-splitting algorithm, proposed in Hugues and Randriamampianina (1998), with a pseudo-spectral Chebyshev method for the spatial discretization. This algorithm has been successfully used in previous studies of binary mixtures in large aspect ratio containers (Batiste *et al*., 2001). The method employs a pressure boundary condition (Karniadakis *et al*., 1991) which in conjunction with stiffly stable schemes, prevents propagation and accumulation of time differencing errors. The Helmholtz and Poisson equations on Chebyshev collocation points resulting from the time splitting are solved efficiently using a complete diagonalization of operators in both directions (Zhao and Yedlin, 1994). Spatial discretization has typically been 90x60 mesh grid points and the time step has been between $\Delta t = 10^{-4}$ and $\Delta t = 5 \times 10^{-5}$. Computations with larger resolution (120x90) or using a smaller time step have been done periodically without producing significant changes, either in the solutions or in the rich diagram of bifurcations presented below.

3. Results

For moderate Rayleigh numbers ($Ra \approx 10^3$) the only stable solution is steady and R-equivariant and consists of a single roll. As the Rayleigh number is increased this roll concentrates in the center, tilts toward the diagonal direction, and develops two weakly co-rotating circulations near the lateral walls of the cavity. This steady solution loses stability at $Ra_c = 1.991 \times 10^3$ in a supercritical Hopf bifurcation that maintains the R-symmetry of the basic solution, so the associated orbits are *F-cycles*. The Hopf frequency is $\omega_c = 6.03$. As a result of this bifurcation, a branch of stable periodic solutions appears. A time sequence of eight

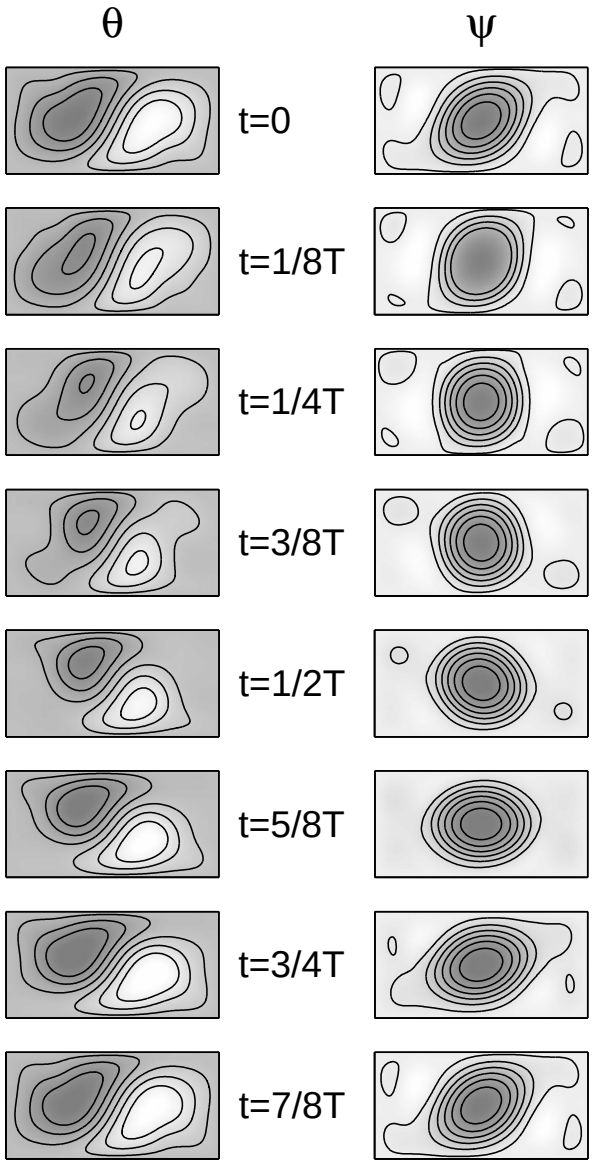

Figure 1. Time sequence of the deviation of the temperature θ and streamlines of the periodic solution at $Ra = 21000$. The period of this solution is $T = 0.29$ in units of vertical thermal diffusion time.

snapshots each one eighth of a period apart, showing the evolution of the deviation of the temperature θ and streamlines for a solution at $Ra = 21000$, is depicted in Fig. 1. The periodic motion hardly affects the core of the roll, which alternates a stretching in the diagonal direction and a circular shape. At the same time small vortices appear and disappear at the corners of the cavity. When the roll stretches, a bigger warm (cold) region settles on the left (right) of the diagonal.

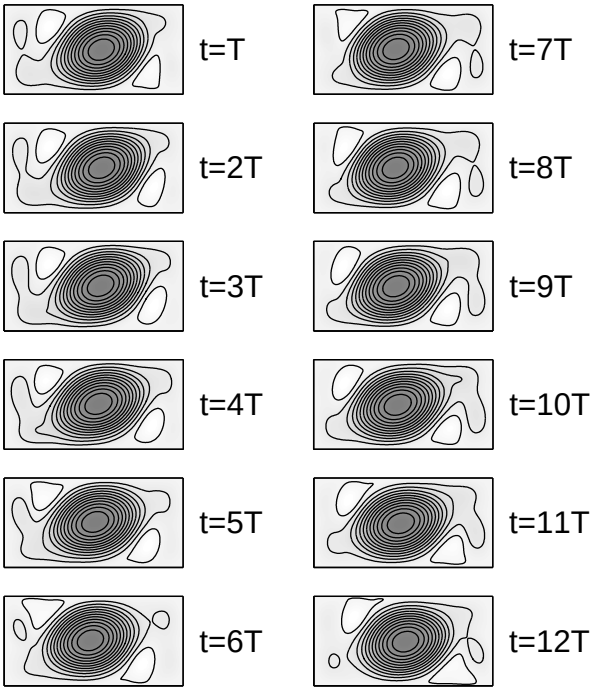

Figure 2. Time sequence of the streamlines of the quasiperiodic solution at $Ra = 22000$. The time interval $T = 1/f_1$ corresponds to the basic frequency $f_1 = 3.59$. The new frequency is $f_2 = 0.29$.

At Rayleigh number $Ra_{NS} \approx 2.11 \times 10^4$, periodic solutions lose stability in a subcritical Neimark-Sacker bifurcation ($f_2 \approx 0.30$), which gives rise to a branch of quasiperiodic states that are no longer invariant under the transformation R. However, the associated orbit is an R-equivariant 2-torus, as predicted by the theory (Kuznetsov, 1985). This means that the orbit associated to the conjugated solution resides on the same torus. The new instability mainly affects the secondary vortices near the lateral walls, which now do not appear symmetrically. This fact can be seen in Fig. 2, where the streamlines of the quasiperiodic solution at $Ra = 22000$ plotted at different instants of time are shown. The frequencies of this solution obtained from the Fourier spectrum are $f_1 \approx 3.59$ and $f_2 \approx 0.29$. The time interval between plots is the period T associated to the basic frequency f_1, and the selected instant corresponds to the stretching of the roll. Notice also that because the ratio between both frequencies is $f_1/f_2 \approx 12$, the streamlines that would correspond to the conjugate solution of that plotted at any instant t resemble those corresponding to the solution at the instant $t + 6T$ (streamlines at the same horizontal level in Fig. 2).

By decreasing the Rayleigh number from Ra_{NS} the quasiperiodic states persist until $Ra \approx 18300$, where a jump to the above mentioned periodic basic solution takes place. When the Rayleigh number is increased, several intervals of frequency locking have been identified. The frequency locking phenomenon is usually associated with Neimark-Sacker bifurcations and is better understood in two parameter families. This bifurcation generically occurs on a one-dimensional curve parametrized by the ratio of the two frequencies associated with the bifurcating torus. From every point of this curve where the ratio of the frequencies is rational ($f_2/f_1 = p/q$), a resonance region (or Arnold tongue) emanates. The boundary of this region consists of two curves of saddle-node bifurcations of periodic orbits. Near the Neimark-Sacker and inside a resonance region, two periodic orbits, one stable and the other unstable, exist on the torus. All trajectories on the torus tend asymptotically to one of these periodic orbits.

We have identified several resonance horns of type $1/q$, and due to the symmetry properties of the basic periodic solution and that of the Neimark-Sacker bifurcation, the periodic solution inside the horn is *symmetric* whenever q is even, and *non-symmetric* when q is odd. This is so because the period of the periodic non R-equivariant solution $\Psi(t)$ in the horn is $T_2 = 1/f_2 = qT_1$, and when q is even $\Psi(t)$ verifies $R\Psi(t) = \Psi(t + qT_1/2) = \Psi(t + T_2/2)$, which is characteristic of the *symmetric* solutions, as commented in Section 2. This is not the case when q is odd. A typical phase diagram (sym, E_k) of a *non-symmetric* periodic solution inside the $1:11$ horn at $Ra = 25110$ is shown in Fig. 4. The stable limit cycles inside the resonance horns lose and gain stability via some typical scenarios in the bifurcation of periodic solutions. We have analyzed in detail all these transitions using Poincaré Section return maps, as described in the following paragraphs.

Since we do not know the exact value of one of the periods as it occurs in periodic forcing systems (Marques *et al*., 2001), in order to build a Poincaré Section, we have fixed a proper value of variable $\theta(P_1)$ when it decreases, and recorded the values of $\beta_n = w(P_1)$ when this occurs. The plot of β_{n+1} versus β_n defines the Poincaré section return maps used here. Very long time integrations have been carried out in order to be sure that the transients have been eliminated in all the time series used. Variable $\theta(P_1)$ has been chosen because its time dependence is smooth, and a value for which the time step between successive impacts was associated to the basic period, is easy to select for it. In addition, in the frequency locking

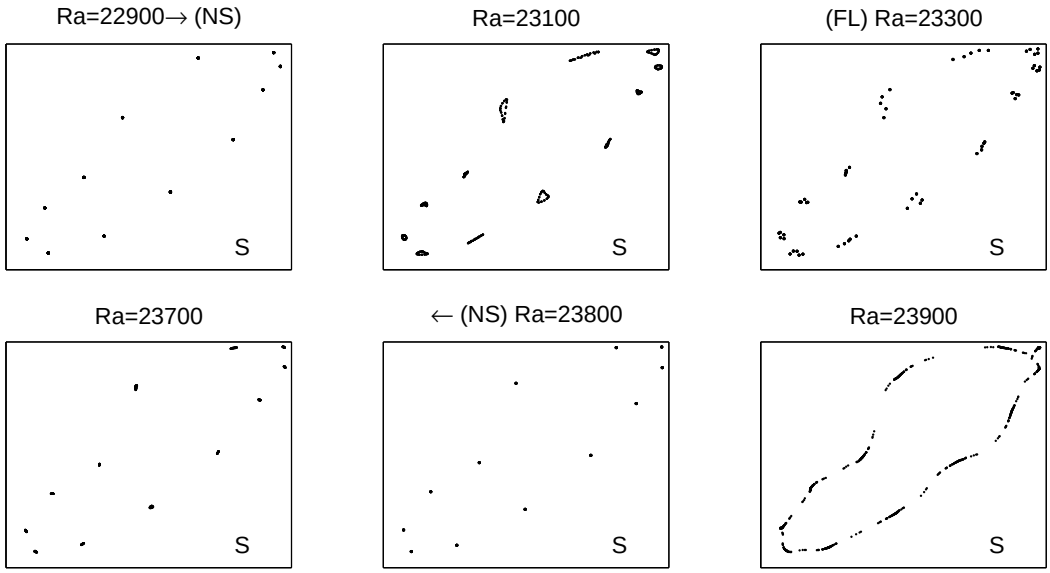

Figure 3. Poincaré Section return maps for solutions of frequencies $f_2/f_1 = 1/12$ obtained for the values of the Rayleigh number indicated in every picture. S indicates a symmetric attractor, NS means a Neimark-Sacker bifurcation and FL a frequency locking phenomenon. Right (left) arrow indicates that a bifurcation appears when the Rayleigh number is increased (decreased).

situation the values of $\beta_n = w(P_1)$ remain far enough apart to enable us to identify clearly the bifurcations that appear inside the resonance horns.

The first resonance horn visited in our one-dimensional path from R_{NS} is a $1:12$ locking. In Fig. 3 we have depicted the Poincaré return maps for the solutions corresponding to different values of the Rayleigh number in this region. An 'S' in a figure is used to indicate a symmetric attractor. For $Ra = 22900$ we obtain the *S-cycle* of the horn. Between this value of the Rayleigh number and $Ra = 23100$, this solution suffers a Neimark-Sacker bifurcation involving a new frequency f_3. At $Ra = 23300$, we observe a frequency locking between f_3 and f_2 of type $f_3/f_2 = 1/5$. At $Ra = 23700$, the quasiperiodic solution of frequencies f_3 and f_2 is again recovered (f_1 is always $12f_2$), and finally at $Ra = 23800$ the *symmetric* cycle is obtained. At $Ra = 23900$ the 1:12 horn has already been left.

After a region of quasiperiodicity that extends to $Ra = 25100$, the horn 1:11 is encountered. The limit cycle in this horn is, as expected, *non-symmetric*. This can be seen at the bottom of Fig. 4, where the phase diagrams (sym, E_k) of different solutions are plotted. Notice how the mentioned phase diagram for the solution at $Ra = 25110$ is no longer symmetric with respect to a vertical line in the middle (the horizontal

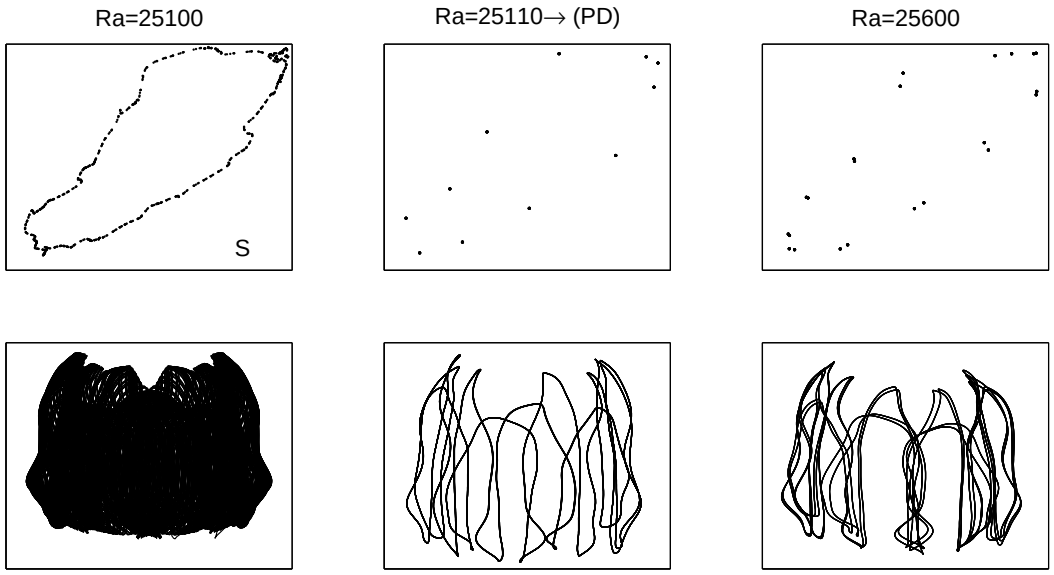

Figure 4. Along the top, Poincaré Section return maps for solutions of frequencies $f_2/f_1 = 1/11$ obtained for the values of the Rayleigh number indicated in every picture. Along the bottom, phase diagrams (sym, E_k) for the solutions corresponding to the Rayleigh number of every picture along the top. The horizontal axis extends between two opposite values of sym. S indicates a *symmetric* attractor, PD means a period doubling bifurcation. The right arrow indicates that a bifurcation appears when the Rayleigh number is increased.

axis of the bottom figures extends between two opposite values of sym), even though the same diagram for the quasiperiodic solution at $Ra = 25100$ certainly is. When the Rayleigh number is increased, at $Ra \approx 25500$, the periodic limit cycle suffers a flip bifurcation (Period doubling), and for $Ra = 25600$ we obtain the solution whose Poincaré return map and phase diagram are plotted in Fig. 4. Remember that in presence of symmetry $\mathbf{Z}_2$ only *F-cycles* and *non-symmetric* cycles may undergo a period doubling. Period doubling bifurcations of the phase-locked limit cycles is one of the typical scenarios of transition to chaos due to torus breakdown according to the Afraimovich-Shilnikov Theorem (Anishchenko *et al*., 1993; Marques *et al*., 2001). This is not the case in our problem.

When the Rayleigh number is increased, at $Ra = 25650$ the torus loses smoothness, but at $Ra = 26000$ we enter a zone where the frequencies f_2 and f_1 are in the ratio $1/10$. The Poincaré return maps of these solutions are plotted in Fig. 5. Among these solutions, only the one at $Ra = 27500$ corresponds to a limit cycle in the Arnold tongue $1:10$, since it is periodic and is an *S-cycle*. A sequence of bifurcations of this solution gives rise to the solutions of the figure, obtained for smaller and higher values of the Rayleigh

number. Thus, the solution at $Ra = 27470$ is a *non-symmetric* cycle appearing from a pitchfork bifurcation that breaks the spacio-temporal symmetry of the solution at $Ra = 27500$. The solution at $Ra = 27400$ comes from a period doubling of the *non-symmetric* solution at $Ra = 27470$, whereas at $Ra = 26890$ we again obtain a *non-symmetric* cycle with the basic period. Further decreasing the Rayleigh number, we obtain at $Ra = 26863$ a solution that stems from a Neimark-Sacker bifurcation of the solution at $Ra = 26890$. The amplitude of the new frequency f_3 is very small and is practically imperceptible in Fig. 5. Notice that in the same picture we have included the return map corresponding to the same Poincaré section for the R-conjugated quasiperiodic solution. This is because we wish to illustrate the gluing bifurcation that takes place between $Ra = 26862$ and $Ra = 26863$. In this homoclinic bifurcation, the two conjugated *non-symmetric* tori ($Ra = 26863$) collide with an unstable *S-cycle* and an R-equivariant torus is obtained ($Ra = 26862$). A detail of the two corresponding pictures of Fig. 5 is shown in Fig. 6.

When, from the solution at $Ra = 27500$, the Rayleigh number is increased, a new frequency f_3 appears through a Neimark-Sacker bifurcation (see the picture for $Ra = 27550$ in Fig. 5), and at $Ra = 27600$ a frequency locking $f_3/f_2 = 1/5$ is observed. From this value the torus breaks down, showing a soft transition to chaos due to the loss of smoothness, as can be seen in the solution for $Ra = 27700$.

However when following the chaotic branch the Rayleigh number increases, we have found that in small intervals the attractor appears to manifest again a quasiperiodic behavior. The Poincaré sections show that at $Ra \approx 30950$ the solution presents a locking $f_2/f_1 = 1/9$ and another frequency f_3 of very small amplitude; and at $Ra \approx 34200$ a solution with a locking $f_2/f_1 = 1/8$ and another frequency is obtained. Similar behavior is observed in the bifurcation sequence leading to the break-up of an invariant torus studied in Aronson *et al*. (1982).

For Rayleigh number $Ra = 35000$, a jump to another branch of quasiperiodic solutions takes place (see Fig. 7). In the same figure we have also shown the Poincaré sections of a solution at a Rayleigh number before the jump and the one corresponding to the new solution. The new solution is quasiperiodic and is not R-equivariant. The Fourier spectrum of the temporal series of a characteristic variable ($u(P_1)$ for example) of the new solution presents peaks at frequencies $f_1, f_1/2$ and $f_1/4$ and at a new frequency f_2, whereas the spectrum of variable sym presents peaks at $f_1/4$ and f_2. According to the Fourier spectra and the Poincaré

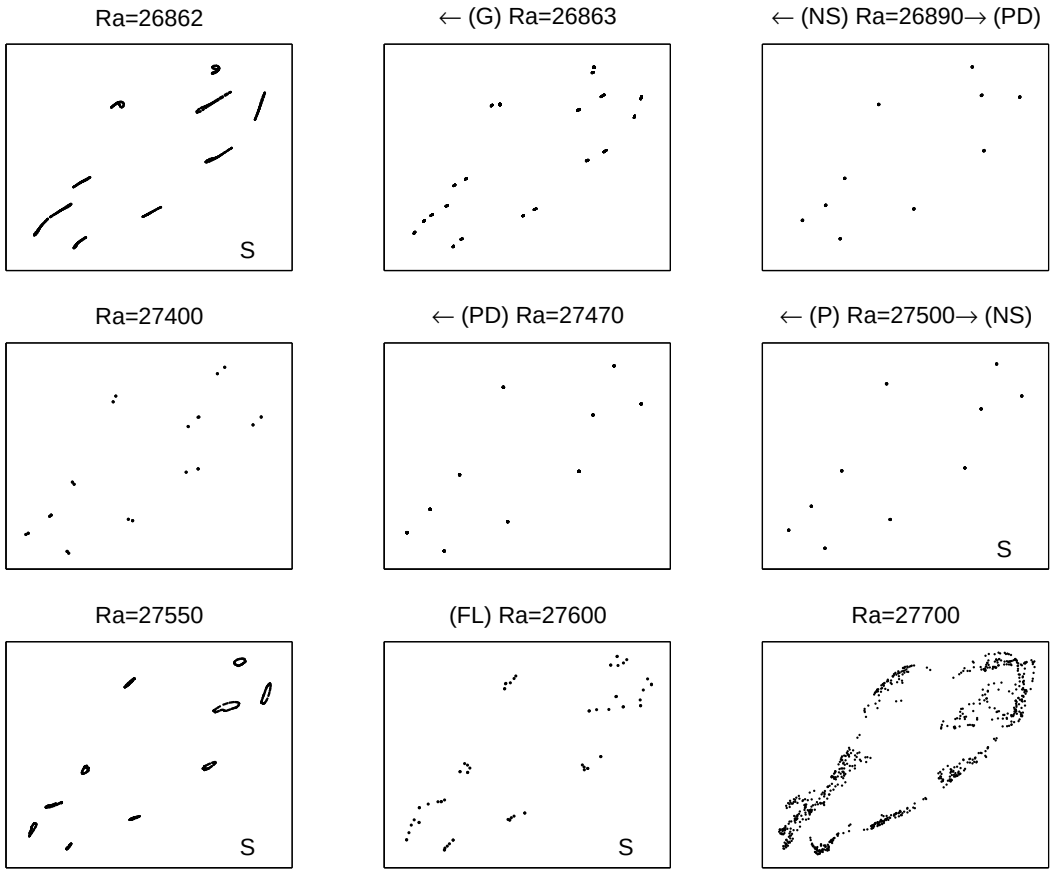

Figure 5. Poincaré Section return maps for solutions of frequencies $f_2/f_1 = 1/10$ obtained for the values of the Rayleigh number indicated in every picture. S indicates a *symmetric* attractor, NS means a Neimark-Sacker bifurcation, P a pitchfork bifurcation, PD a period doubling, G a gluing bifurcation, and FL a frequency locking phenomenon. In the picture corresponding to $Ra = 26863$, the Poincaré Section return map for the conjugated solution is also included. Right (left) arrows indicate that a bifurcation appears when the Rayleigh number is increased (decreased).

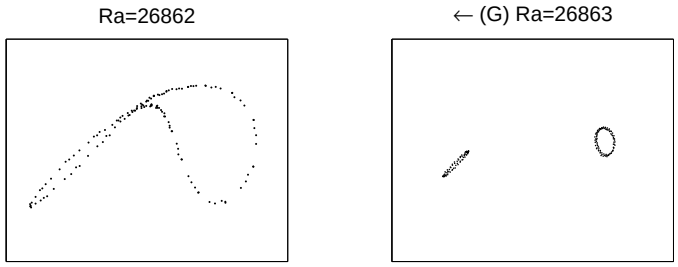

Figure 6. Detail of the Poincare Section return maps for solutions at $Ra = 26862$ and $Ra = 26863$ depicted in the previous figure, where we can appreciate the gluing bifurcation mentioned in the text.

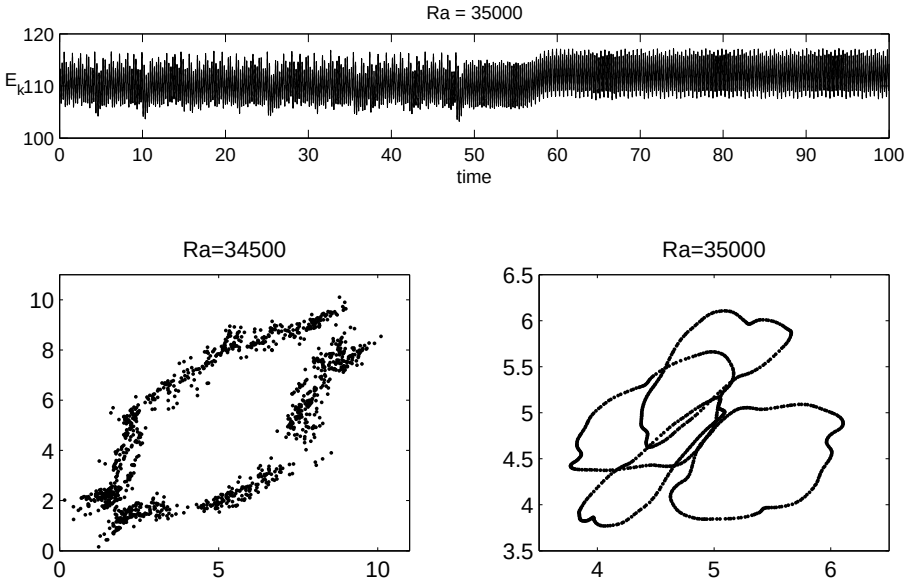

Figure 7. Transition between two families of quasiperiodic solutions. Top: Time series of the kinetic energy E_k for a solution at $Ra = 35000$ showing the jump. Bottom: Poincaré section return maps for two solutions belonging to the different branches at $Ra = 34500$ (before the jump) and $Ra = 35000$.

section we suppose that the new solutions come from two successive period doubling bifurcations of the basic *F-cycle*, the first one maintaining the symmetry, and the second one breaking it (this would justify the peak of sym at $f_1/4$) and later, a Neimark-Sacker bifurcation of frequency f_2. By forcing the symmetry, we have been able to localize a supercritical period doubling bifurcation of the basic periodic solution which takes place at $Ra \approx 26700$, but we have not been able to establish a clear connection between the new branch and this bifurcation since the connecting branches, if they exist, are unstable. The dynamics of the new branch and that of other branches found for higher, and even for smaller, values of the Rayleigh number seems to be dominated by the interaction between the Neimark-Sacker bifurcation described in this paper and the flip bifurcation mentioned above. Deeper analysis is required for greater understanding of this dynamics and it will be the subject of a forthcoming paper.

4. Summary and Conclusions

In this paper we present a detailed study of the transition to chaos in the problem of convection of a small Prandtl number fluid ($\sigma = 0.00715$), confined in a rectangular cavity ($\Gamma = 2$) with lateral heating. The study in the parameter space is one-dimensional, since all parameters are fixed except the Rayleigh number. The different solutions obtained in this work have been analyzed taking into account the symmetry group of the system, $\mathbf{Z}_2$, which influences both the type of bifurcations that can appear and the bifurcated solutions. We have obtained a route to chaos via quasi-periodicity and frequency locking in resonance horns, leading to torus break-up.

The quasiperiodic solutions come from a subcritical Neimark-Sacker bifurcation that breaks the symmetry of a branch of R-equivariant periodic solutions. In spite of the well-known fact that quasiperiodic solutions may not persist away from the secondary Hopf bifurcation, in this problem they do so in a significant region ($18300 < Ra < 27000$). Before the destruction of the torus the system passes through various resonances horns. Inside these horns we have obtained solutions that appear via some typical bifurcations of the limit cycles, including global bifurcations. The transition to chaos due to torus breakdown can be made, according to the Afraimovich-Shilnikov theorem (Anishchenko *et al*., 1993), via three different scenarios: 1) breakdown due to some typical bifurcations of the phase-locked limit cycle, 2) abrupt transition to chaos in the homoclinic region via saddle-node bifurcation of the phase-locked limit cycle and 3) soft transition to chaos due to the loss of torus smoothness. Our results appear to be related to scenario 3.

We have compared our results with those in previous papers devoted to studying the states that appear from the onset of unsteadiness in laterally heated cavities. Among these papers, we will refer first to the work of Pulicani *et al*. (1990) as representative of the study of a similar fluid contained in more elongated cells. Pulicani *et al*. (1990), who considered a cavity of aspect ratio $\Gamma = 4$ and Prandtl number $\sigma = 0$, obtained a sequence of bifurcations that led to quasiperiodic states, which was similar to ours (except for the subcritical character of our Neimark-Sacker bifurcation). However, our results differ from this point. A periodic solution with the flow pattern changing alternately between two and three roll cells was obtained and, finally, for higher values of the Rayleigh number, the only stable state was a steady solution with two

co-rotating rolls. The different behaviour may be attributed to the different aspect ratio considered. The greater length of the container allows a different number of rolls to fit in it, and the instabilities arising from this fact dominate over other types of instabilities such as those obtained in our smaller box. Time dependent states are also described in detail in the work of Le Quéré and Behnia (1998), in which a square cavity with adiabatic horizontal walls filled with air ($\sigma = 0.71$) is considered. The authors obtained that the first bifurcation of the basic R-equivariant solution, which takes place at a very high value of the Rayleigh number (stabilizing effect of the smaller value of the aspect ratio), is a Hopf bifurcation that breaks the symmetry, in contrast to our case. The transition to chaos seems also to be associated to a quasiperiodic route. We have also analyzed the transition to chaos in the same system, imposing adiabatic boundary conditions on the horizontal plates (the results will be presented in a forthcoming paper), and we can anticipate that in spite of the small value of the Prandtl number, the dynamics obtained from the first bifurcation differs considerably. In conclusion, we confirm the strong dependence of the dynamics on the aspect ratio, on the Prandtl number and on horizontal boundary conditions commented in the introduction.

References

Anishchenko V.S., Safonova M.A., and Chua L.O., *IEEE Trans. Circuits Sys.–I* **40**, (1993) 792–800.

Aronson D., Chory M., Hall G. and McGehee R., *Comm. Math. Phys.* ,**83**, (1982) 303–354.

Batiste O., Knobloch E., Mercader I. and Net M., *Phys. Rev. E*, **65** 016303, (2001) 1–19.

Braunsfurth M.G., Skeldon A.C., Juel A., Mullin T. and Riley D.S., *J. Fluid Mech.*, **342**, (1997) 295–314.

Gelfgat A. Y., Bar-Yoseph P.Z. and Yarin A.L., *J. Fluid Mech.* **388**, (1999) 315–334.

Hugues S. and Randriamampianina A., *Int. J. Numer. Methods Fluids*, **28**, (1998) 501–521.

Juel A., Mullin T., Ben Hadid H. and Henry D., *J. Fluid Mech.*,**436**, (2001) 267–281.

Karniadakis G. E., Israeli M. and Orszag S.A., *J. Comput. Phys.*, **97**, (1991) 414–443.

Kuznetsov Y.A., *Elements of Applied Bifurcation Theory*. (Applied Mathematical Sciences, Springer-Verlag 1985).

Le Quéré P. and Behnia M., *J. Fluid Mech.* **359**, (1998) 1–107.

Marques F., Lopez J.M. and Shen J., *Physica D*, **156**, (2001) 81-97.

Pulicani J.P., Crespo del Arco E., Randriamampianina A., Bontoux P. and Peyret R., *Intl. J. Num. Meth. Fluids* **10**, (1990) 481–517.

Xin S. and Le Quéré P., *Phys. Fluids* **13** (9), (2001) 2529–2542.

Yahata H., *J. Phys. Soc. Jpn.* **68** (2), (1999) 446–460.

Zaho S. and Yedlin M. J., *J. Comput. Phys.*, **113**, (1994) 215–223.